GEOLOGICA CARPATHICA, DECEMBER 2011, 62, 6, 489–500 doi: 10.2478/v10096-011-0035-6

Clay mineralogy of the Paleozoic-Lower Mesozoic sedimentary sequence from the northern part of the Arabian Platform, Hazro (Diyarbakır, Southeast Anatolia)

ÖMER BOZKAYA[1*], HÜSEYIN YALÇIN[1] and HÜSEYIN KOZLU[2]

[1]Cumhuriyet University, Department of Geological Engineering, TR-58140 Sivas, Turkey; *bozkaya@cumhuriyet.edu.tr
[2]Niğde Caddesi, 18/1, Dikmen/Ankara, Turkey

(Manuscript received November 15, 2010; accepted in revised form June 9, 2011)

Abstract: The Paleozoic–Lower Mesozoic units in the Diyarbakır-Hazro region consist of sandstone (subarkose, quartz arenite), mudstone, shale, coal, marl, dolomitic marl, limestone (biomicrite, lithobiosparite, biosparite with lithoclast, dololithobiosparite, dolomitic cherty sparite) and dolomite (dolosparite, dolosparite with lithoclast, biodolosparite with glauconite). These units exhibit no slaty cleavage although they are oriented parallel to bedding planes. The sedimentary rocks contain mainly calcite, dolomite, quartz, feldspar, goethite and phyllosilicates (kaolinite, illite–smectite (I–S), illite and glauconite) associated with small amounts of gypsum, jarosite, hematite and gibbsite. The amounts of quartz and feldspar in the Silurian-Devonian units and of dolomite in the Permian-Triassic units increase. Kaolinite is more commonly observed in the Silurian-Devonian and Permian units, whereas illite and I–S are found mostly in the Middle Devonian and Triassic units. Vertical distributions of clay minerals depend on lithological differences rather than diagenetic/metamorphic grade. Authigenetic kaolinites as pseudo-hexagonal bouquets and glauconite and I–S as fine-grained flakes or filaments are more abundantly present in the levels of clastic and carbonate rocks. Illite quantities in R3 and R1 I–S vary between 80 and 95 %. $2M_1$+$1M_d$ illites/I–S are characterized by moderate *b* cell values (9.005–9.040, mean 9.020 Å), whereas glauconites have higher values in the range of 9.054–9.072, mean 9.066 Å. KI values of illites (0.72–1.56, mean 1.03 $\Delta 2\theta°$) show no an important vertical difference. Inorganic (mineral assemblages, KI, polytype) and organic maturation (vitrinite reflection) parameters in the Paleozoic-Triassic units agree with each others in majority that show high-grade diagenesis and catagenesis (light petroleum-wet gas hydrocarbon zone), respectively. The Paleozoic-Triassic sequence in this region was deposited in the environment of a passive continental margin and entirely resembles the Eastern Taurus Para-Autochthon Unit (Geyikdağı Unit) in respect of lithology and diagenetic grade.

Key words: geochemistry, mineralogy, diagenesis, phyllosilicate.

Introduction

Paleozoic-Early Mesozoic parts of the Arabian Platform or Southeast Anatolian Autochthon (SEAA) (Göncüoğlu et al. 1997) unit crop out in the Amanos, Diyarbakır-Hazro and Hakkari-Çukurca regions, from west to east (Fig. 1). The Hazro area is one of the important potential petroleum basins in Turkey, known as an anticline structure (Hazro anticline). It comprises the best preserved and continuous outcrops of Middle Paleozoic-Lower Mesozoic sequences. Many studies focused on the general and petroleum geology were conducted in this area (e.g. Tolun 1951; Yahşıman & Ergönül 1959; Kellog 1960; Schmidt 1964; Ağralı & Akyol 1967; Lebküchner 1976; Güven et al. 1982; Bozdoğan et al. 1987; Çubukçu & Sayılı 1990; Perinçek et al. 1991). In addition to these, a detailed book related to the stratigraphic lexicon of SEAA units was published by the geologists of the Turkish Petroleum Company (Yılmaz & Duran 1997).

The determination of diagenetic — very low-grade metamorphic characteristics of the Paleozoic aged sedimentary rocks by means of the textural and mineralogical (crystallinity, polytype, *b* cell dimension) properties could supply valuable data related to tectonic setting of the sequence and paleogeographic evolution of a region (e.g. Merriman & Frey 1999; Merriman & Peacor 1999; Merriman 2005). These types of studies were done during the past decade in Southern Turkey and provided new scientific contributions to the interpretation of the evolution of the Taurus Belt (e.g. Bozkaya & Yalçın 2000, 2004a,b, 2005, 2010; Bozkaya et al. 2002, 2006). The aim of this study is to describe the diagenetic degree by means of clay mineralogy of the Paleozoic-Lower Mesozoic sedimentary rocks of SEAA units from the Arabian Platform, and to obtain some additional data related to petroleum maturity zones.

Stratigraphy and lithology

Paleozoic-Early Mesozoic successions in the Hazro area contain rock units called the Diyarbakır, Tanin and Çığlı Groups which are divided into several formations and were named in earlier studies (Schmidt 1964; Bozdoğan et al. 1987; Perinçek et al. 1991; Yılmaz & Duran 1997) (Fig. 2). The Silurian–Early Triassic aged Diyarbakır Group is made up of Dadaş (Upper Silurian–Lower Devonian), Hazro (Lower Devonian) and Kayayolu (Middle–Upper Devonian) Formations. The Tanin and Çığlı Groups comprise Kaş and Gomaniibrik (Upper Permian) and Yoncalı, Uludere and Uzungeçit (Lower Triassic) Formations, respectively.

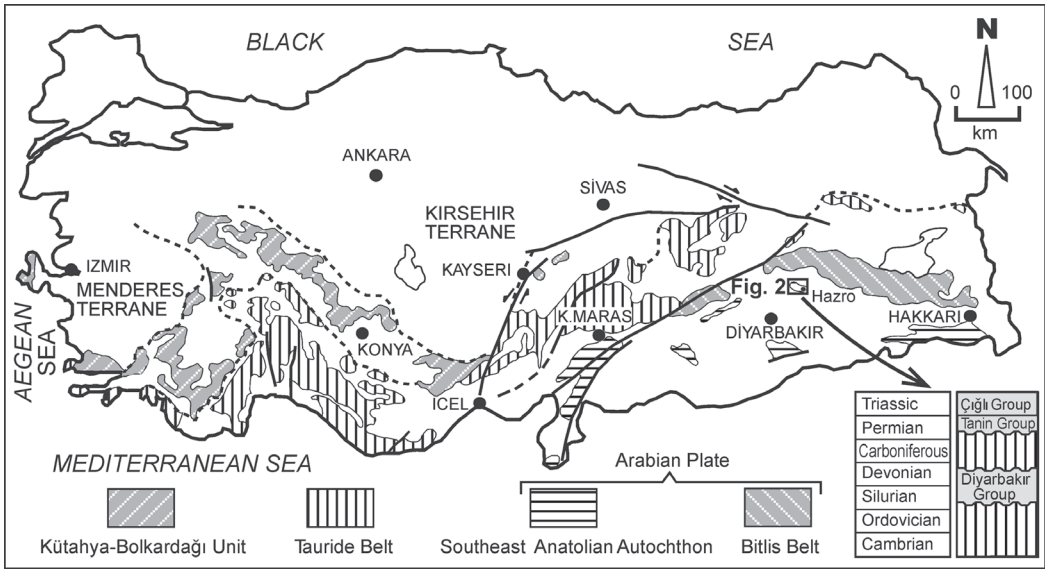

Fig. 1. Tectonic units of southern Turkey (Göncüoğlu et al. 1997) and vertical distributions of the Paleozoic–Lower Mesozoic units in the Hazro area.

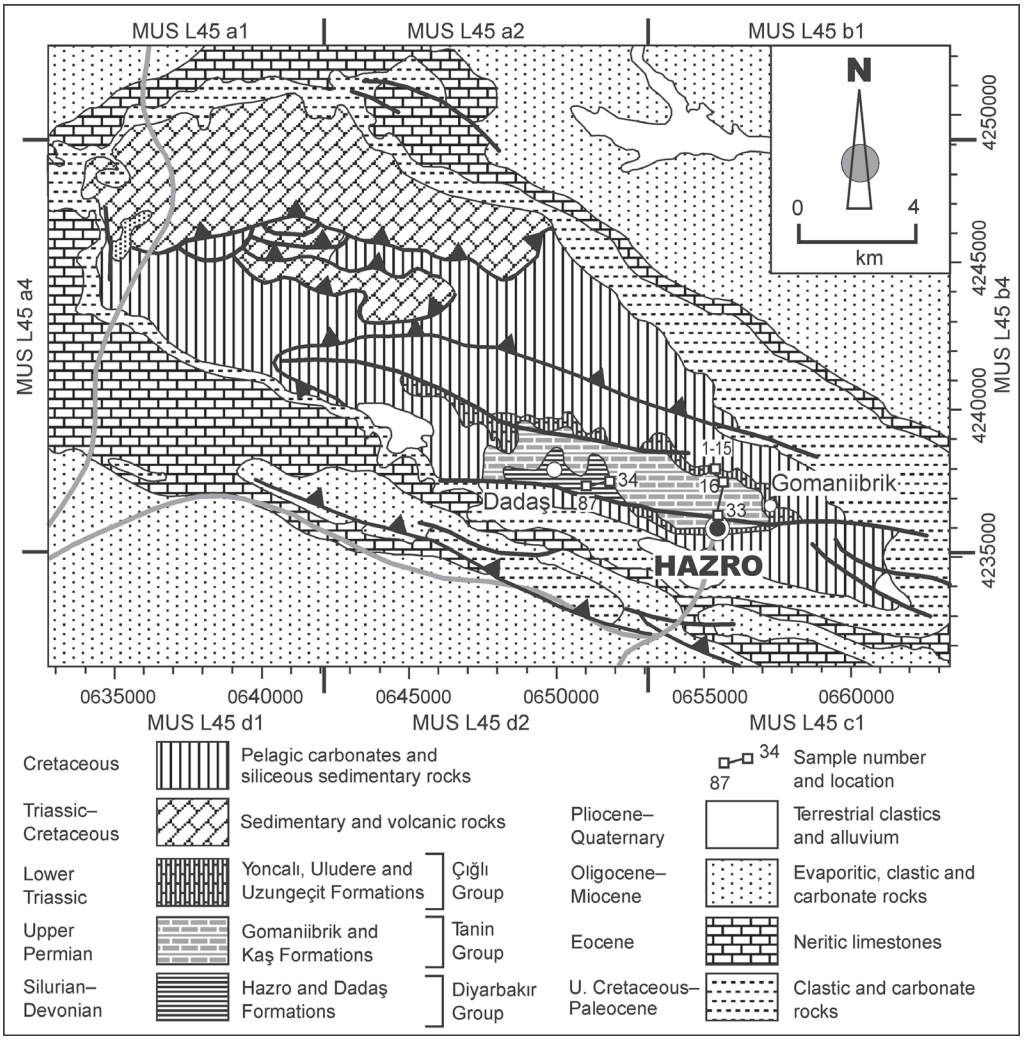

Fig. 2. Geological map of the Hazro area (MTA 2002).

The Dadaş Formation, the lowermost unit in the area, crops out in the rims of the anticline, is an approximately 80 m thick sedimentary sequence of Late Silurian–Early Devonian age (Bozdoğan et al. 1987). It comprises mainly of shale, siltstone, mudstone and sandstone with rarely limestone intercalations. The organic matter types and contents of this formation are evaluated as a potential source rock for petroleum occurrence (Bozdoğan et al. 1987).

The Early Devonian aged Hazro Formation which crops out only in the Hazro area, is conformably overlain by the Dadaş Formation, and involves different lithologies in the lower, middle and upper parts of the sequence. The lower and middle parts of the formation are formed from dolomitic marls with dolomite intercalations and mudstone, sandstone and marls. The upper parts are made up of marls intercalated with poorly cemented sandstones with petroleum and dolomite lithologies.

The Late Permian aged Kaş Formation discordantly overlies the Hazro Formation, and includes coal measures within the quartz arenitic sandstones and coaly shales. High contents of spores and pollen are characteristic for this formation (Ağralı & Akyol 1967). Coaly levels are formed by four zones with various thicknesses, namely 1.00, 0.15, 0.30 and 1.00 m.

The Late Permian aged Gomaniibrik Formation is passed to the Çığlı Group with conformable boundary and divided into three facies: A, B and C (Bozdoğan et al. 1987). The A, and C facies are composed of carbonate rocks, whereas B facies is made up of siliciclastic rocks. Carbonate levels include fossiliferous limestone, dolomite, dolomitic marl and clayey dolomites. Limestones are characterized by plentiful neritic fossils. Petroleum leakages were first observed in the fissures of dolomites during the field studies. Siliciclastic levels are represented by sandstone, mudstone and shale lithologies.

The Yoncalı, Uludere and Uzungeçit Formations of Çığlı Group are of Early–Middle Triassic age (Köylüoğlu 1986), and include mainly shale, limestone, dolomite, dolomitic marl and sandstone lithologies. Brownish-green shales with claret red sandstone interlayers in the lower levels are characteristic of the Triassic units, as stated by Açıkbaş (1978) for the Hakkari-Uludere area. Limestones with brachiopods, pinky dolomite, and green glauconite patched sandy limestone, white-pink sandstone and dolomitic marls were observed in the middle levels of the Çığlı Group, whereas dolomite, sandstone and dolomitic shales were found in the upper levels of the Çığlı Group.

Materials and methods

A total of 90 samples was collected along the measured stratigraphic sections, and analysed by optical (OM) and scanning electron (SEM) microscopy, vitrinite reflection (VR) and X-ray diffraction (XRD) methods.

VR measurements were fulfilled on the coal and organic matter-rich samples through polished blocks by Orthoplan microscope (Leitz-Wetzlar MPV-II) in the Department of Geological Engineering, Hacettepe University (Ankara, Turkey).

XRD analyses were done using a Rigaku DMAX IIIC diffractometer in the Department of Geological Engineering, Cumhuriyet University (Sivas, Turkey). The diffractometer conditions were arranged as CuKα (1.541871 Å), Ni filter, 35 kV, 15 mA, speed of goniometer =0.5°/min, step 0.01°, 0.02°, 0.04°, time constant = 1 and 4 sec, slits = 1° 0.15 mm, 1° 0.30 mm, 2θ interval = 2θ = 2–30°, 5–35°, 59–63°, 5–65°, 16–32°. The semi-quantitative mineral amounts in the bulk and clay fraction (<2 μm) of sedimentary rocks were calculated by the external method of Brindley (1980a).

Clay separation was done by the sedimentation method after chemical dissolution (removing carbonate minerals), deflocculation and sedimentation during 3 hours 40 minutes for 200 ml clay suspension. Clay mud was mounted on glass and subjected to air-drying, glycolating (16 h under 60 °C) and heating (4 h under 490 °C) procedures before the XRD studies.

Identification of clay minerals, ordering types (R0, R1, R3) and illite contents of illite–smectite (I–S) were determined by the method of Moore & Reynolds (1997).

Illite "crystallinity" measurements were performed on the first peaks of illites (10 Å), as the width of half of the peak height (Kübler index (KI) — Kübler 1968; Guggenheim et al. 2002). Standard samples of Warr & Rice (1994) were used for calibration (e.g. Bozkaya et al. 2006). In this study, KI values were obtained from decomposed illite peaks owing to co-existing illite and I–S peaks as broad and asymmetrical shapes. Because of the asymmetrical nature of illite peaks in the presence of I–S, KI values were measured from the symmetrical extension of illite peaks, as reflected from the right sides of the peaks to their left sides. KI values were correlated to full width half maximum (FWHM) results of decomposed peaks from X-ray diffractograms in which illite peaks could be separated from I–S peaks, and an equation ($KI = 0.669 \times FWHM + 0.056$, $r^2 = 0.82$) was obtained for conversion of FWHM to KI values.

The 211 peak (2θ = 59.97°, d = 1.541 Å) of quartz was taken as the reference for the measurement of the d_{060} values of illites. The regression equation of Hunziker et al. (1986) was used for the octahedral Mg+Fe contents of illite/muscovites. Polytype examinations were investigated for illite and kaolinite through representative peaks proposed by Bailey (1988). Illite polytype proportions were calculated by peak area ratios of Grathoff & Moore (1996). Peak areas were individually determined on the fitted peaks by the WINFIT program (Krumm 1996). Illite percentages in I–S were calculated from Moore & Reynolds (1997). 2θ or d_{001} values were detected from the decomposed peaks by the WINFIT program. The results were also correlated with the calculated patterns of the NEWMOD program (Reynolds 1985).

Results

Optical microscopy

On the basis of representative samples from the Paleozoic-Lower Mesozoic sequence, the shales and siltstones in the Dadaş Formation of Late Silurian–Early Devonian age contain quartz, feldspar, sericite, muscovite and high amounts of organic matter in some samples. Shales have sericitized clay matrix and serve micro-lamination (0.3–1.0 mm) and micro-orientation (Fig. 3a). Limestones with sparitic orthochems include micritic intraclasts and fossil shells. In addition to extraclasts of quartz, feldspar and mica, rare glauconite occurrences were also

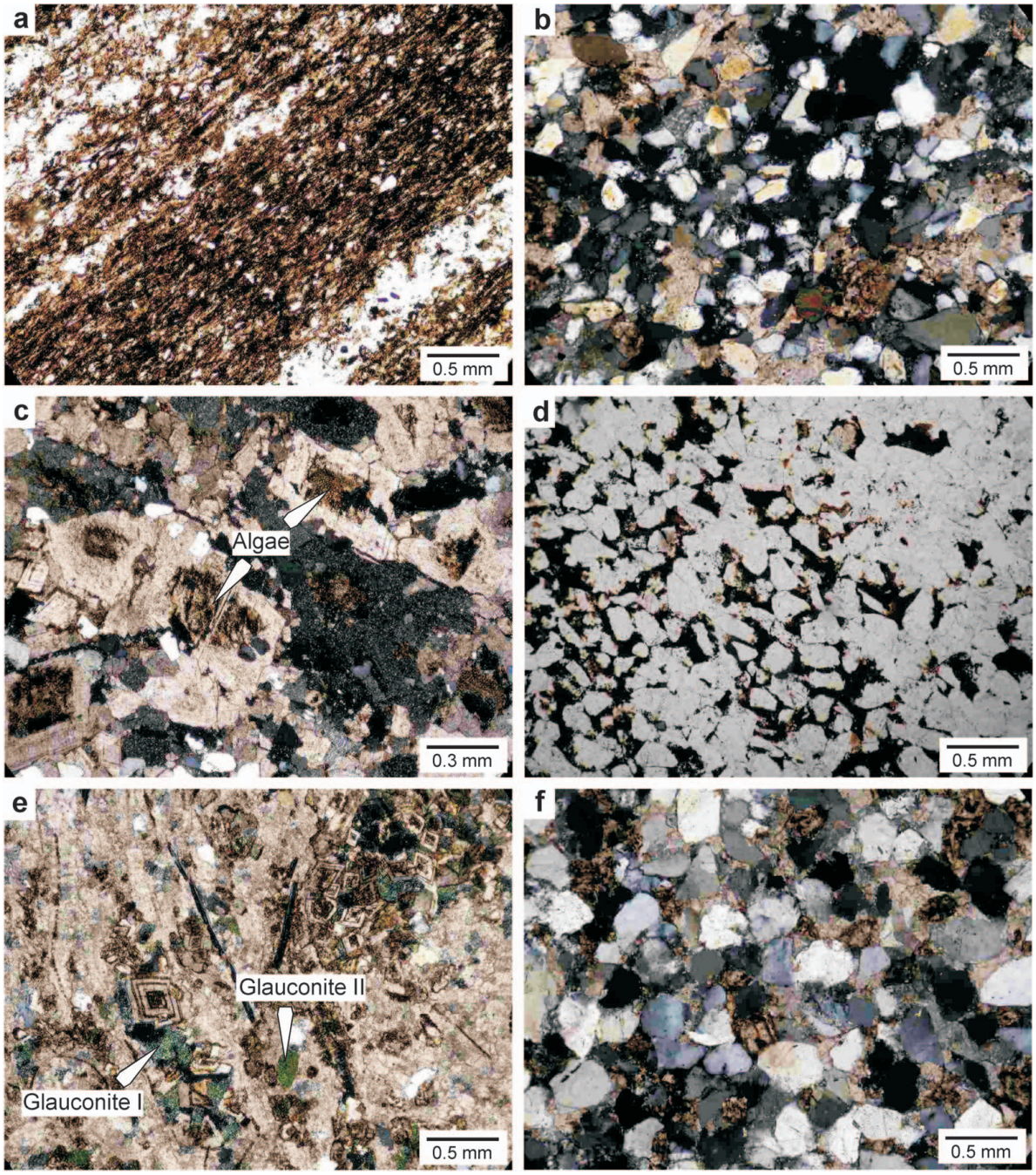

Fig. 3. Optical microscopic characteristics of the representative rock samples: **a** — Quartz- and organic matter-rich micro laminations in the siltstones from Mardin-Derik area (MDK-90, Dadaş Formation, Silurian, parallel nicols); **b** — Well-sorted quartz and feldspar grains in the subarkose with sparicacite cement in Hazro area (DBH-80, Dadaş Formation, Silurian–Devonian, crossed nicols); **c** — Euhedral dolomites surrounding algae fragments in the dolosparites in the Hazro area (DBH-71, Hazro Formation, Middle Devonian, crossed nicols); **d** — Well sorted subrounded-subangular quartz grains in the quartz arenites with iron-oxide cement (DBH-44, Kaş Formation, Upper Permian, parallel nicols); **e** — Authigenic glauconites (type I) surrounding euhedral dolomites with zoned texture and roundish-ellipsoidal grains (type II) in biodolosparite (DBH-12, Yoncalı Formation, Triassic, parallel nicols); **f** — Well sorted subangular-subrounded quartz grains without any orientation in the quartz arenite with sparicalcite cement (DBH-15, Yoncalı Formation, Triassic, parallel nicols).

observed in the limestone with biosparitic and lithointrabiosparitic composition (Folk 1968). Carbonate cemented subarkosic sandstones with medium-poor sorting have higher amounts of quartz, feldspar (plagioclase, microcline), biotite, and muscovite than siltstone and mudstones (Fig. 3b).

In the Lower Devonian Hazro Formation, silica cemented quartz arenites are composed of mainly subangular-subrounded quartz, and scarce feldspar, calcite and zircon, and show poorly sorting. Silty shales and mudstones contain sericitized clay matrix and dolomite cement in addition to quartz and

feldspar grains. Carbonate rocks with sparitic orthochems (dolosparite, dolomitic cherty lithosparite, dololithobiomicrosparite) display coarse subhedral-euhedral dolomite, chalcedonic quartz and glauconite minerals. Algae fragments were marked in the cores of the euhedral dolomite crystals in some samples (Fig. 3c).

In the Upper Permian Kaş Formation, quartz arenites signify no orientation texture, and contain mainly quartz and feldspar and accessory muscovite, tourmaline, zircon and apatite. The groundmass material is formed by iron-oxide minerals (hematite) in some sandstones (Fig. 3d).

In the Upper Permian Gomaniibrik Formation, the limestones have biomicritic characteristics. The dolomites have coarse-grained sparitic and partly microsparitic dolomite crystals. The medium sorted and poorly cemented sandstones have subangular-subrounded quartz grains without orientation.

In the Yoncalı, Uludere and Uzungeçit Formations of the Çığlı Group of Early–Middle Triassic age, sandy limestones (lithosparite, glauconite-bearing lithosparite and lithobiosparite) cover quartz, feldspar, accessory muscovite, apatite, tourmaline, zircon, goethite and opaque minerals as extraclasts. Spherical-ellipsoidal granular glauconite occurrences within the pores of carbonate rocks are typical of the Triassic units. Limestones (biosparite, glauconite-bearing biosparite) and dolomites (dolosparite, glauconite-bearing biodolosparite, and lithoclast-bearing biodolosparite) contain euhedral and zoned dolomite and glauconite (as pore filling and roundish-ellipsoidal) occurrences in addition to fossil shells (Fig. 3e). Sandstones (subarkose, quartz arenite) with sparry calcite cement have mono- and poly-crystalline quartz and feldspar (zoned plagioclase) grains without any orientation (Fig. 3f).

Scanning electron microscopy

This investigation was performed on the six samples including carbonate and clay minerals. Illites and illite-rich I–S minerals are observed as coarse flakes and ribbon-like filaments (5–10 μm) (Fig. 4a), whereas illite-poor I–S are seen as relatively fine curved flakes (Fig. 4b). Hexahedral shaped jarosites and their traces are also noticed together with illite-poor I–S in the coaly shale samples. Kaolinites show the classic platy, pseudo-hexagonal accordion- or book-like forms indicating typical au-

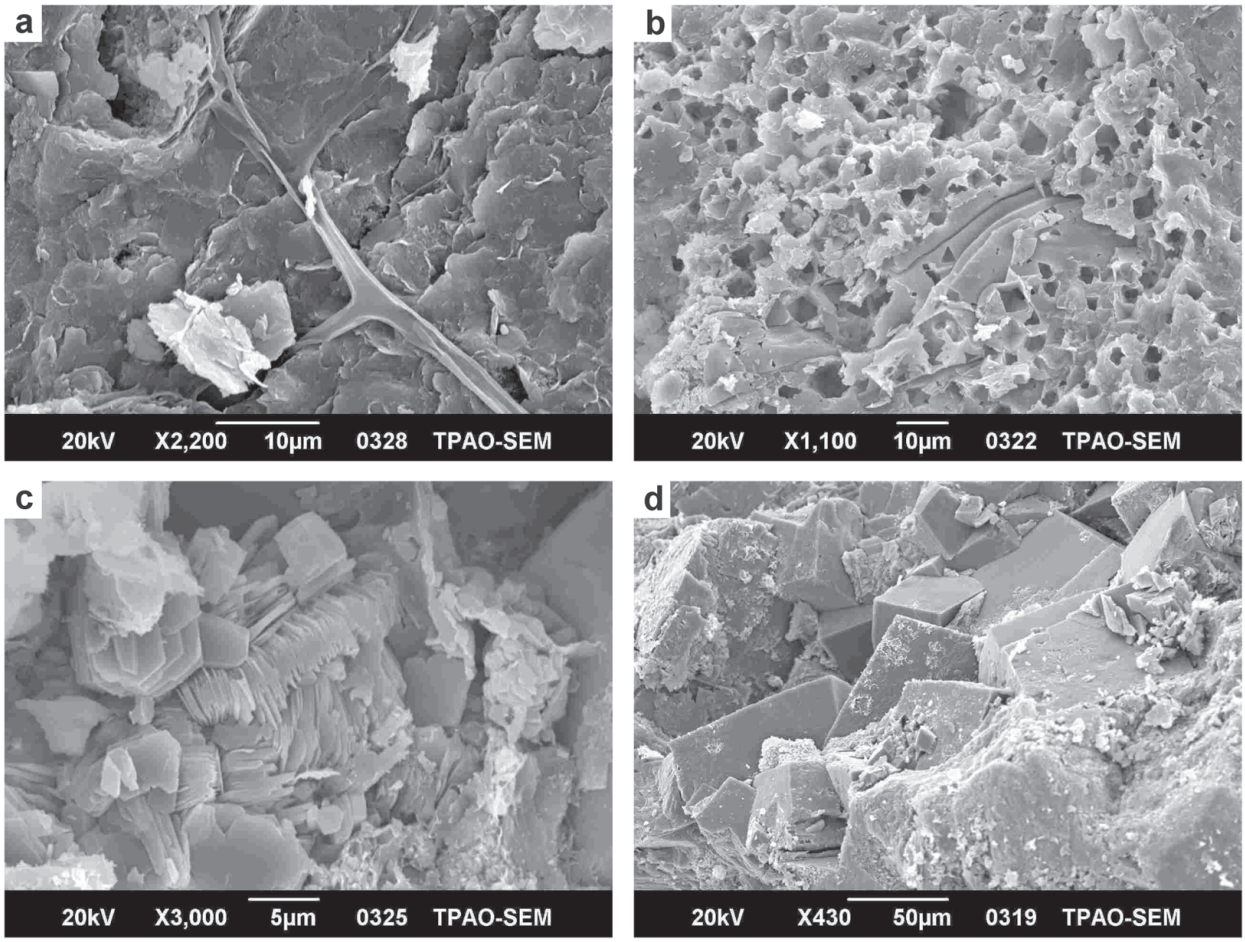

Fig. 4. SEM photomicrographs of the samples: **a** — Illite and illite-rich I–S aspects as long filaments and coarse flakes, respectively, in shales (DBH-81, Dadaş Formation, Silurian–Devonian); **b** — Illite-poor I–S as fine curved flakes associated with hexahedral jarosites in the coaly shales (DBH-35, Kaş Formation, Upper Permian); **c** — Euhedral pseudo-hexagonal shaped kaolinite crystals with tightly packaged book-like form and I–S as coarse flakes in sandstones (DBH-76, Dadaş Formation, Silurian–Devonian); **d** — Rhombohedral dolomite crystals and glauconites as fine-grained thin flakes on the dolomites (DBH-12, Yoncalı Formation, Triassic).

thigenetic occurrences (Fig. 4c). The tight package of kaolinite booklets reflects a high grade of diagenesis. Euhedral dolomites show typical rhombohedral morphologies in carbonate rocks (Fig. 4d). Clay occurrences as thin flakes were shown on the dolomite crystals. Illite was found not only as fine-grained flakes, but also as ribbon-like filaments.

Organic petrography

According to organic petrographic investigations on a shale sample of the Silurian Dadaş Formation in the Derik area and a coal sample of the Kaş Formation in the Hazro area; the main components (macerals) are represented by vitrinite, tellinite and inertinite. Vitrinites are shown as thick and thin bands without any inner texture, whereas tellinites have a plant texture. Inertinites are characterized by light grey colours in addition to plant texture as sieve (Fig. 5).

VR values in the samples of the Dadaş and Kaş Formations, collected from the Derik and Hazro regions, respectively, are measured as 1.32–2.29 Rm_{oil} % (mean 1.75) and 0.49–0.66 Rm_{oil} % (mean 0.55) for Dadaş and Kaş Formations (Fig. 6). These values correspond to low volatile bituminous and sub-bituminous coal ranks of USA classification (Teichmüller 1987), and their coalification ranks are consistent with the catagenesis or high diagenetic grades (Merriman & Frey 1999).

X-ray mineralogy

Bulk and clay mineralogy

The Silurian-Triassic sedimentary units in the study area are formed of quartz, feldspar, calcite, dolomite, goethite, hematite, jarosite, gypsum, gibbsite and clay (illite, kaolinite, I–S) minerals. The most common clay mineral associations are illite + I–S and kaolinite + illite + I–S (Fig. 7). Illite and I–S with different ordering types show the composed peaks with broad and asymmetrical shapes. Individual peaks were decomposed by the WINFIT program, and correlated and/or confirmed by calculated patterns created by the NEWMOD program (Fig. 8).

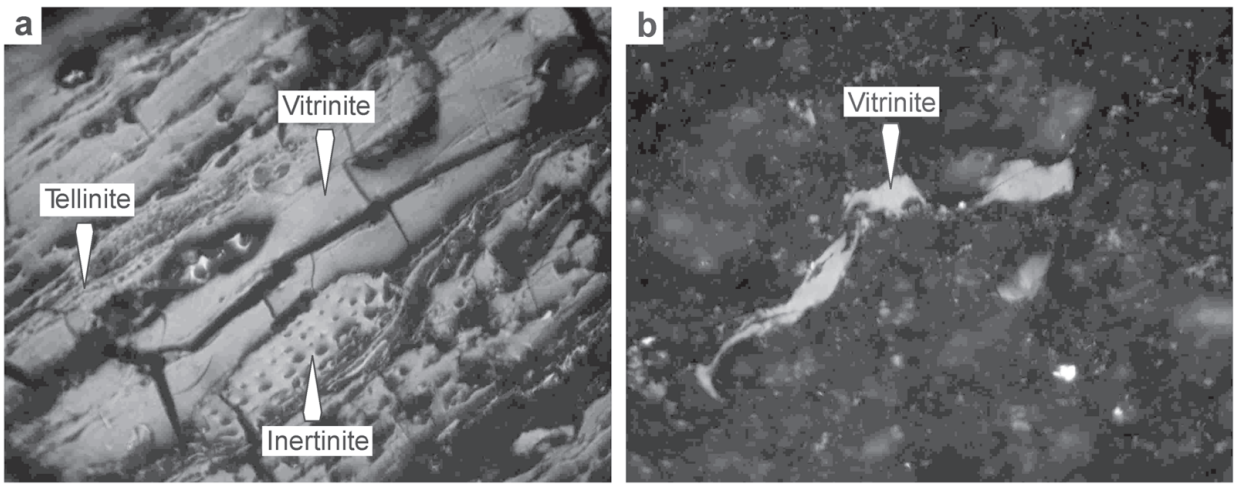

Fig. 5. Microscopic appearances of main maseral types: **a** — Coal sample of the Kaş Formation (DBH-42, Hazro area); **b** — Shale sample of the Dadaş Formation (MDK-89, Derik area).

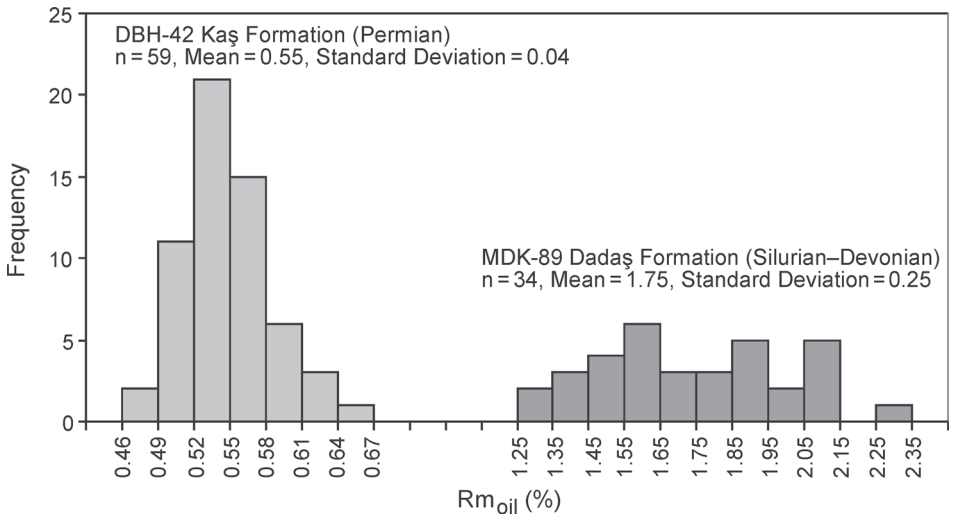

Fig. 6. The frequency distribution of VR values measured in the samples of coal (DBH-42) and shale (MDK-89).

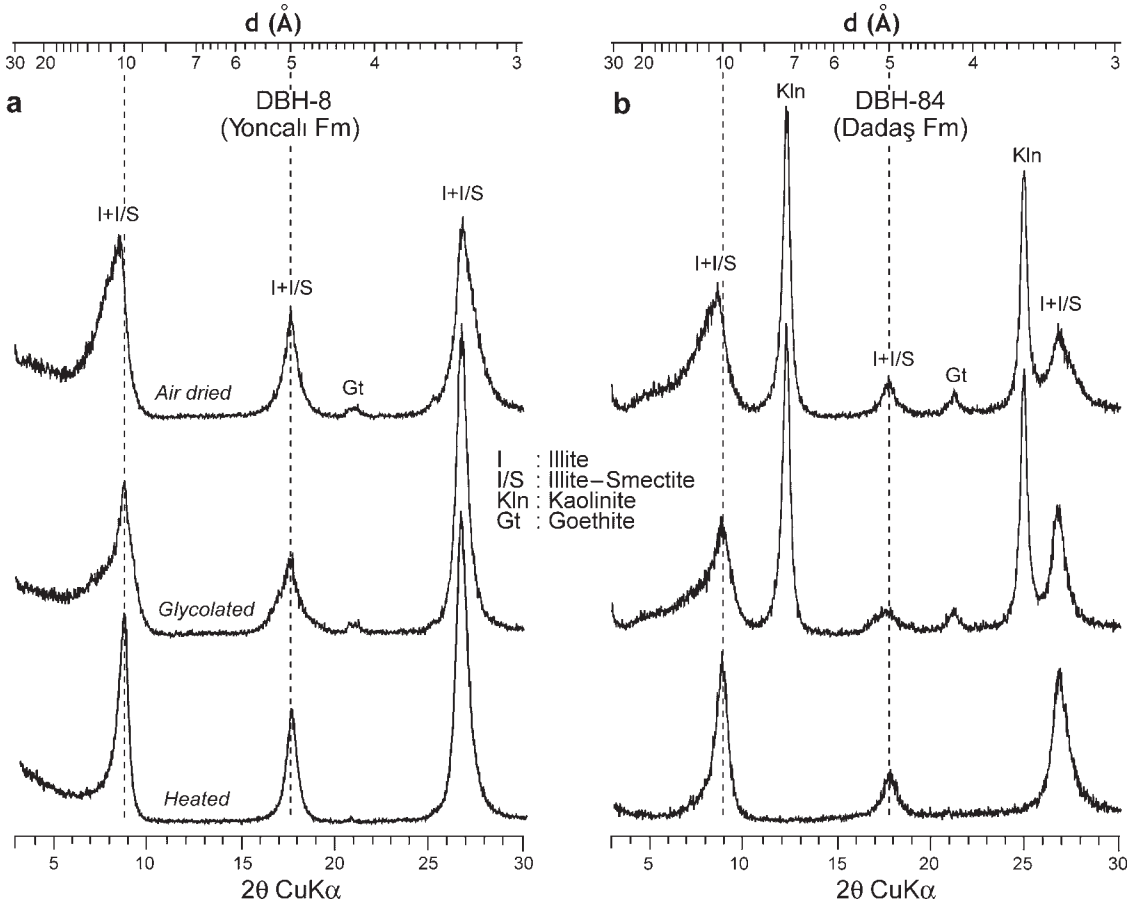

Fig. 7. XRD patterns of the typical clay mineral assemblages in the Hazro area: **a** — Illite+I–S; **b** — Kaolinite+illite+I–S.

According to decomposed peaks and their correlations with calculated patterns, I–S minerals with both R1 and R3 ordering type accompany the illite. The illite contents of R1 and R3 I–S are 70–85 % and 90–95 %, respectively. R0 I–S is rare and found only in two calcareous rocks of Triassic units. Glauconite-bearing samples have R3 type glauconite–smectite (G–S) ordering in addition to glauconite. The smectite contents of G–S from pore-filling authigenic and round-shaped granular types are measured as 13 % and 10 %, respectively.

Crystal-chemical characteristics of clay minerals

The KI values, both measured directly on illite 10 Å peaks and converted from the FWHM values of decomposed illite 10 Å peaks (Fig. 9), vary between 0.77–1.56 (Δ2θ°) for Silurian-Triassic samples from the Hazro area (Table 1), and reflect low and high diagenetic conditions. However, KI values for Silurian samples in the Mardin area range from 0.50 to 0.62 (Δ2θ°), and indicate completely high diagenetic con-

Table 1: Mineralogical properties of illite/I–S and glauconites (Italic values represent glauconite samples).

Unit	Age	KI (Δ°2θ) (mean)	d_{060} (Å) (mean)	$2M_1/(2M_1+1M_d)$	R0	R1	R3	N (nm) (mean)
Yoncalı	Triassic	0.81–1.14 (1.00) *0.81–0.90 (0.86)*	1.5033–1.5053 (1.5041) *1.509–1.512 (1.511)*	55 *1M*	50 –	75–80 –	90 *87–90*	7–10 (9) *7–8 (8)*
Kaş	Permian	–	–	–	–	75	90	–
Gomaniibrik	Permian	0.81–1.40 (1.03)	1.5008–1.5043 (1.5028)	35	–	70–80	90	6–11 (9)
Hazro	Devonian	0.72–1.28 (0.93)	1.5013–1.5067 (1.5046)	40	–	75–85	90	7–13 (10)
Dadaş	Silurian–Devonian	0.77–1.56 (1.16)	1.5028–1.5053 (1.5041)	40	–	75–85	90–95	7–11 (8)
	Silurian	0.50–0.62 (0.56)	1.5003–1.5013 (1.5008)	45	–	85	95	12–14 (13)

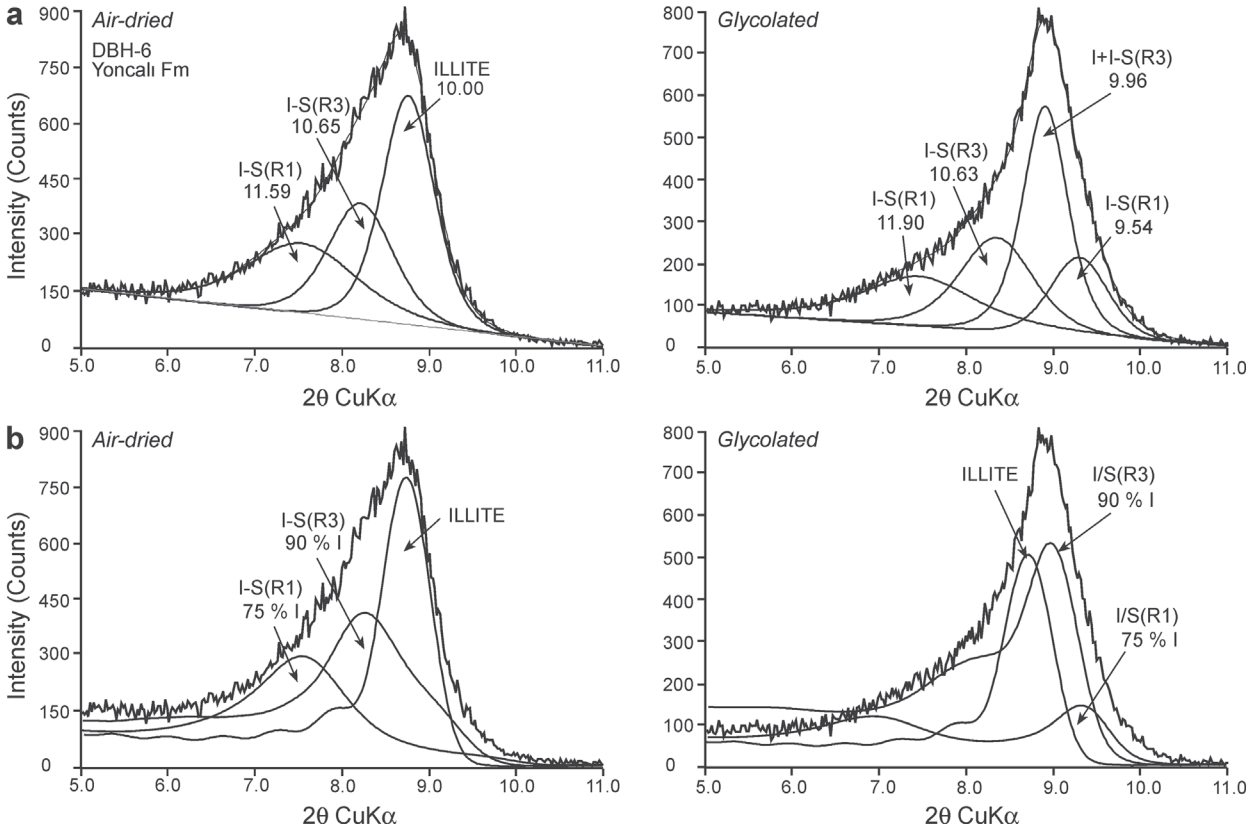

Fig. 8. Decomposition of compound peaks of illite and I–S by means of **a** — WINFIT and **b** — NEWMOD© programs.

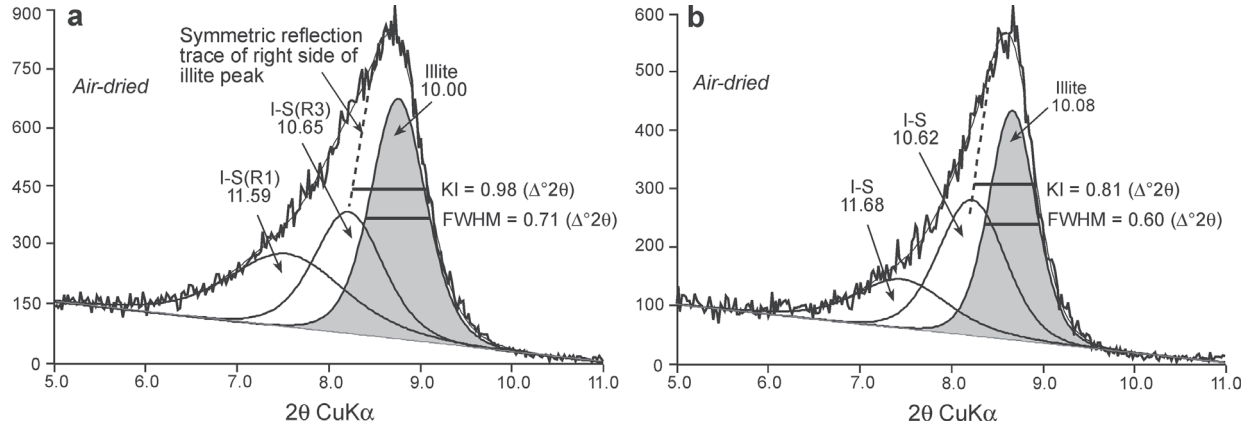

Fig. 9. Decomposition of illite +R1 and R3 I–S peaks and FWHM and KI values of illites obtained from resolved and unresolved 10 Å peak by assuming symmetrical reflection of the right-side of the peak: **a** — Dolomitic shale of Yoncalı Formation (Triassic); **b** — Dolomitic marl of Gomaniibrik Formation (Permian).

ditions. The KI values of pore-filling authigenic and round-shaped granular glauconites are determined as 0.81 and 0.90 (Δ2θ°), respectively.

In addition to illites, the FWHM (Δ2θ°) values of decomposed peaks of R1 and R3 I–S are also measured together with their d_{001} (Å) values (Fig. 10). In general, decreasing FWHM values accompany decreasing d_{001} (Å) values, as a result of regular transformation from smectite-rich I–S to illite. Although the KI values show no remarkable differences between the formations, some were due to lithological varieties (Fig. 11). Illites from clay-rich lithologies have generally higher KI values than those of carbonate-rich lithologies. Crystallite size (*N*) values, calculated from XRD peaks using the WINFIT program, vary between 6 and 14 nm (Table 1), and indicate low- to high-grade diagenesis. Silurian samples from the Mardin area indicate the highest crystallite size values, reflecting relatively higher diagenetic grades, similar to the KI values.

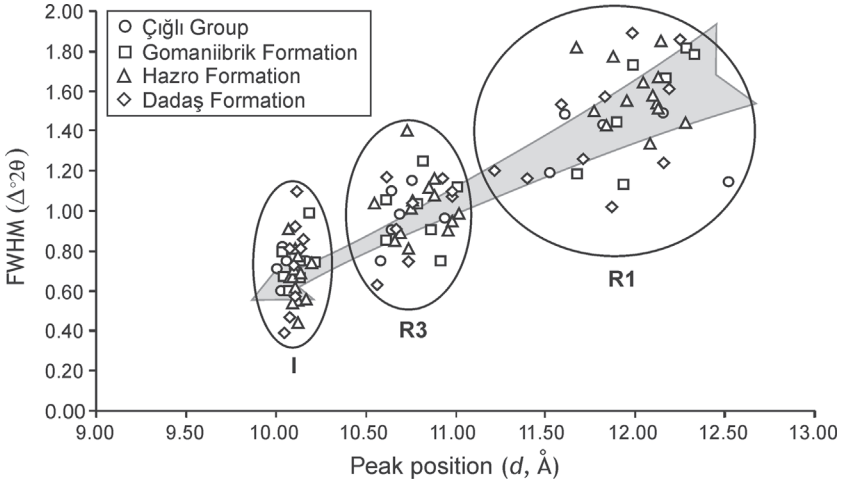

Fig. 10. Variations of width and positions of decomposed peaks in illite and I–S (arrow shows a direction of progressive transformations from R1 I- to illite).

In the Hazro area, the $d_{(060)}$ values of illite and I–S minerals vary in a broad interval of 1.5008–1.5053 Å, which correspond to octahedral Fe+Mg contents of 0.35–0.58, indicating the composition of phengite-rich white K-mica. Silurian samples from the Dadaş Formation in the Mardin area have relatively lower $d_{(060)}$ values (Table 1), and point to muscovite-rich composition (Fe+Mg content is 0.35). The $d_{(060)}$ values of granular and pore-filling glauconites are determined as 1.5092 and 1.5115 Å, respectively, which are close to those of the ideal glauconite (1.512–1.517 Å; Brindley 1980b).

Illite/I–S shows $2M_1$ (35–45 %) and $1M_d$ (55–65 %) polytypes for Permian and older units, and $2M_1$ (55 %) and

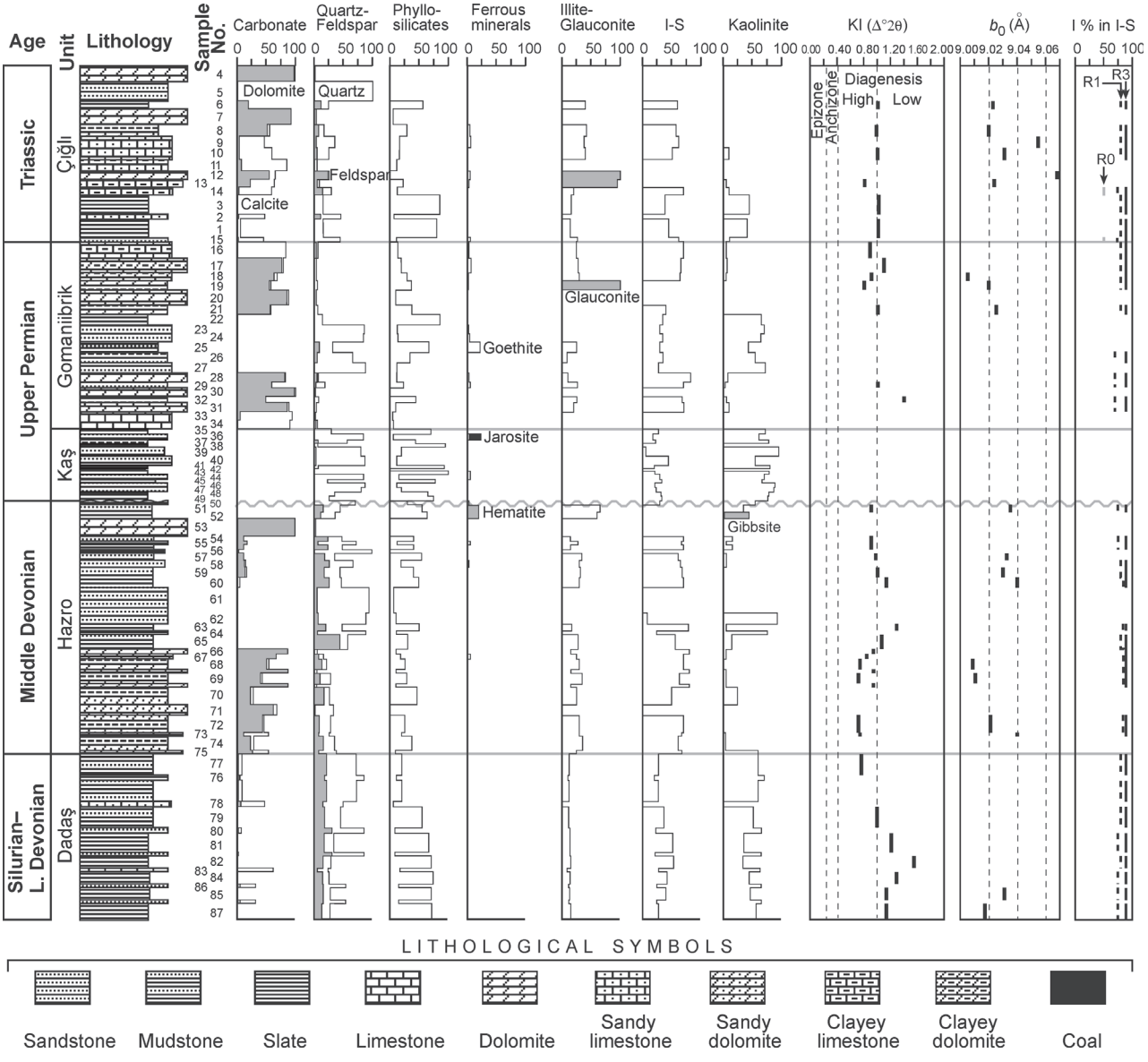

Fig. 11. Vertical distributions of bulk and clay mineral distributions with some mineralogical parameters in the Hazro area.

$1M_d$ (45 %) for Triassic units. Glauconite and kaolinite have completely $1M$, and $1T$ kaolinite polytype with respect to the representative peaks.

Discussion

Vertical distributions of clay minerals

Bulk and clay minerals show relatively different abundances and assemblages in respect to the vertical distributions (Fig. 11). Quartz and feldspar are found in higher amounts in the Silurian–Lower Devonian units, whereas the dolomite content is high in Middle Devonian–Triassic units. Goethite in Upper Permian–Triassic, hematite and gibbsite in Devonian, jarosite in Devonian–Upper Permian and gypsum in Triassic units are detected. Kaolinite is decisive in the Silurian–Devonian and Upper Permian, whereas I–S is dominant in the Lower Devonian and Triassic in higher amounts. Glauconite is encountered only in Triassic units. The mineralogical distributions in the studied units are related to lithological differences rather than to age and maturation, thus kaolinite is found in higher amounts in the clastic-rich lithologies, but I–S is rich in carbonate-rich lithologies.

Origin and occurrences

Although the abundances of illite and kaolinite depend upon the lithological variations, as kaolinite and illite are respectively dominant in clastic- and carbonate-rich lithologies, they have diagenetic (authigenic) rather than of detrital origin. Their diagenetic origin was confirmed by the presence of glauconite, dominance of sericitized groundmass, the absence or negligible amounts of detrital micas and clay shapes (flake, filament and euhedral pseudo-hexagonal booklets).

In addition to the fabric properties of the studied rock samples, the crystal-chemical characteristics of illite and I–S (KI, dominance of $1M_d$ polytype), illite contents of I–S, firmly packaged kaolinite booklets and vitrinite reflectance data indicate their occurrence under high-grade diagenetic conditions. The peak position (Å) and FWHM ($\Delta 2\theta°$) values of illite and I–S (R1 and R3) show a regular distribution from R1 I–S to illite; this indicates a progressive transformation of smectite to illite. Thus, the association of illite, R1 and R3 I–S indicates that illites have a diagenetic origin rather than being inherited from fine-grained detrital micas. This approach was also confirmed by the presence of I–S in quite low amounts in the clastic-rich lithologies.

Glauconite firstly detected in Triassic rocks during this study is an indicator for marine environments (e.g. Tucker 2001; Flügel 2004), and indicates a relatively shallow environment (shelf) with a low-rate of sedimentation (Amorosi 1995; Chafetz & Reid 2000; El Albani et al. 2005). It is observed within the pores in the carbonate-rocks and roundish or ellipse-shaped intra-clastic particles in the extraclast-bearing carbonate rocks. These textural relationships indicate the glauconites were developed in-situ (authigenic) and transported within the same basin (e.g. Amorosi 1993). According to mineralogical variations of the different types of glauconites (Fig. 3e), they have a relatively regular ordering compared to transported glauconites because of the defecting crystal-chemical structures during transportation. Additionally, the current and ancient glauconite-bearing carbonate rocks have significant differences that limit a decisive use of the medium shelf-deep water or low-sedimentation-rate environments (e.g. Chafetz & Reid 2000; El Albani et al. 2005).

Paleogeographic and tectonic settings

The studied series reflect almost homogeneous deposition and lithification under low- to high-grade diagenetic conditions. In these types of sequences, which had not suffered intense diagenesis/metamorphism, the vertical and lateral distributions of clay minerals can be used to describe the depositional history of the sedimentary rocks (e.g. Chamley 1989; Inglès & Anadon 1991; Inglès & Ramos-Guerrero 1995). In general, clay mineral assemblages in ancient sequences are controlled by lithology, depositional environments, paleoclimate and topography, etc. Clay mineral associations (kaolinite, illite/I–S, glauconite) in the Paleozoic–Lower Mesozoic sequence in the Hazro area mainly exhibit post-burial (diagenetic) conditions rather than detrital input. According to optical- and electron-microscopic observations, both kaolinite and I–S are completely of authigenetic origin, and were precipitated within the pores during diagenesis. The dominance of kaolinite seems to be related to a depositional environment close to low latitudes under tropical climate conditions (e.g. Biscaye 1965; Griffin et al. 1968).

Stratigraphic-lithological, textural and mineralogical data from the Paleozoic–Lower Mesozoic sedimentary units in the Hazro area introduce the sediment accumulation and diagenesis in a shallow marine environment without major volcanic and tectonic activities. Inorganic and organic maturation remains at the diagenetic level, which indicates the typical passive margin conditions (e.g. Robinson 1987). In addition to these, iron-(hydr)oxide minerals, phengitic illite and glauconite occurrences represent iron-rich neoformed clays, which are also characteristic for shallow shelf environments within the passive continental marginal basins (Merriman 2005). Both stratigraphic-lithological and mineralogical characteristics of the sequence offer significant similarities to the Paleozoic-Mesozoic sequence of the Eastern Tauride Belt (Bozkaya et al. 2002; Bozkaya & Yalçın 2004b), that represents a typical passive continental margin.

Conclusions

The Silurian-Triassic sequence from the Hazro region includes carbonate and clastic rocks with roughly fabric orientation parallel to bedding without cleavage, which shows textural maturation of diagenetic grade. According to mineralogical data, the carbonate and clastic rocks mainly contain calcite, dolomite, feldspar, goethite and phyllosilicate (kaolinite, illite, I–S, glauconite), and rarely gypsum, jarosite, hematite and gibbsite. The vertical distributions of minerals are seen to be related to lithology rather than diagenetic maturation. The presence of hematite-jarosite in the Silurian-De-

vonian and goethite and gypsum in the Permian–Triassic units indicate that oxidation or shallow environmental conditions are dominant for the younger units.

Regarding the clay mineralogical distribution, clastic-rich lithologies (sandstone, siltstone) contain high amounts of authigenetic euhedral kaolinite crystals as cement and pore filling that indicate a period of erosion under high energy conditions with high detrital input and indirectly the relatively low pH conditions. However, carbonate-rich lithologies (dolomite, limestone, marl) represent relatively low-energy conditions with sporadic detrital input under the high pH condition, so they contain high amounts of I–S. In other words, the organic data and crystal-chemical characteristics of phyllosilicate minerals indicate high diagenetic conditions and show no remarkable differences through the sequence.

Consequently, mineralogical distributions in the sequence are related to variations of lithological and/or micro-environmental conditions, and the units were deposited and petrified on a passive margin setting under tropical climate conditions, so that they resemble the Eastern Taurus Autochthon (Geyikdağı Unit, Özgül 1976) from southern Turkey.

Acknowledgments: This study is supported by the Scientific Research Found of Cumhuriyet University under the project number M-235. The authors thank Fatma Yalçın (Cumhuriyet University) for laboratory studies, Dr. A. İhsan Karayiğit (Hacettepe University) for measurements of organic-matter reflectance, Tuğrul Tüzüner (Turkish Petroleum Corporation) and other technical staff for electron microscope investigations. We are grateful to two anonymous referees for reviews and suggesting valuable comments.

References

Açıkbaş D. 1978: Geology and hydrocarbon possibilities of Çukurca-Köprülü-Yığınlı (Hakkari) areas. [Çukurca-Köprülü-Yığınlı (Hakkari ili) alanının jeolojisi ve hidrokarbon olanakları.] *Turkish Petroleum Corporation Search Group Report,* 2303, 67 (in Turkish).

Ağralı B. & Akyol E. 1967: Etüde Palynologique des charbons de Hazro et considerations sur l'age des horizons lacustres du Permo–Carbonifere. *Miner. Res. Explor. Inst. Turkey Bull.* 68, 1–26 (in Turkish).

Amorosi A. 1993: Use of glauconites for stratigraphic correlation: a review and case studies. *Giornale di Geologia* 55, 117–137.

Amorosi A. 1995: Glaucony and sequence stratigraphy: a conceptual framework of distribution in siliciclastic sequences. *J. Sed. Res.* B65, 419–425.

Bailey S.W. 1988: X-ray diffraction identification of the polytypes of mica, serpentine, and chlorite. *Clays Clay Miner.* 36, 193–213.

Biscaye P.E. 1965: Mineralogy and sedimentation of recent deep-sea clay in the Atlantic Ocean and adjacent seas and oceans. *Geol. Soc. Amer. Bull.* 76, 803–832.

Bozdoğan N., Bayçelebi O. & Willink R. 1987: Paleozoic stratigraphy and petroleum potential of Hazro area, S.E. Turkey. *Turkish 7th Petroleum Congress*, *Proc.*, 117–130 (in Turkish).

Bozkaya Ö. & Yalçın H. 2000: Very low-grade metamorphism of Upper Paleozoic–Lower Mesozoic sedimentary rocks related to sedimentary burial and thrusting in Central Taurus Belt, Konya, Turkey. *Int. Geol. Rev.* 42, 353–367.

Bozkaya Ö. & Yalçın H. 2004a: New mineralogical data and implications for the tectono-metamorphic evolution of the Alanya Nappes, Central Tauride Belt, Turkey. *Int. Geol. Rev.* 46, 347–365.

Bozkaya Ö. & Yalçın H. 2004b: Diagenetic to low-grade metamorphic evolution of clay mineral assemblages in Palaeozoic to early Mesozoic rocks of the Eastern Taurides, Turkey. *Clay Miner.* 39, 481–500.

Bozkaya Ö. & Yalçın H. 2005: Diagenesis and very low-grade metamorphism of the Antalya Unit: Mineralogical evidences on the Triassic rifting, Alanya-Gazipaşa, Central Taurus Belt, Turkey. *J. Asian Earth Sci.* 25, 109–119.

Bozkaya Ö. & Yalçın H. 2010: Geochemistry of mixed-layer illite-smectites from an extensional basin, Antalya unit, Southwestern Turkey. *Clays Clay Miner.* 5, 644–666.

Bozkaya Ö., Yalçın H. & Göncüoğlu M.C. 2002: Mineralogic and organic responses to the stratigraphic irregularities: an example from the Lower Paleozoic very low-grade metamorphic units of the Eastern Taurus Autochthon, Turkey. *Schweiz. Mineral. Petrogr. Mitt.* 82, 355–373.

Bozkaya Ö., Gürsu S. & Göncüoğlu M.C. 2006: Textural and mineralogical evidence for a Cadomian tectonothermal event in the eastern Mediterranean (Sandıklı-Afyon area, western Tauides, Turkey). *Gondwana Res.* 10, 301–315.

Brindley G.W. 1980a: Quantitative X-ray mineral analysis of clays. In: Brindley G.W. & Brown G. (Eds.): Crystal structures of clay minerals and their X-ray identification. *Mineral. Soc. London*, 411–438.

Brindley G.W. 1980b: Order-disorder in clay mineral structures. In: Brindley G.W. & Brown G. (Eds.): Crystal structures of clay minerals and their X-ray identification. *Mineral. Soc. London*, 125–195.

Chafetz H.S. & Reid A. 2000: Syndepositional shallow-water precipitation of glauconite minerals. *Sed. Geol.* 136, 29–42.

Chamley H. 1997: Clay mineral sedimentation in the ocean. In: Paquet H. & Clauer N. (Eds.): Soils and sediments mineralogy and geochemistry. *Springer*, Berlin, 269–302.

Çubukçu A. & Sayılı A. 1990: Authigenic clays of the Hazro Formation sandstone in south Hazro field. *Turkish 8th Petroleum Congress*, *Proc.*, 305–313 (in Turkish).

El Albani A., Meunier A. & Fürsich F. 2005: Unusual occurrence of glauconite in a shallow lagoonal environment (Lower Cretaceous, northern Aquitane Basin, SW France). *Terra Nova* 17, 537–544.

Flügel E. 2004: Microfacies of carbonate rocks: analysis, interpretation and application. *Springer*, Heidelberg, 1–976.

Folk R.L. 1968: Petrology of sedimentary rocks. *Hemphill's*, Austin–Texas, 1–170.

Göncüoğlu M.C., Dirik K. & Kozlu H. 1997: General characteristics of pre-Alpine and Alpine Terranes in Turkey: explanatory notes to the terrane map of Turkey. *Ann. Géol. Pays Hellén.* 37, 515–536.

Grathoff G.H. & Moore D.M. 1996: Illite polytype quantification using Wildfire© calculated X-ray diffraction patterns. *Clays Clay Miner.* 44, 835–842.

Griffin J.J., Windom H. & Goldberg E.D. 1968: The distribution of clay minerals in the world oceans. *Deep-Sea Res.* 15, 433–459.

Guggenheim S., Bain D.C., Bergaya F., Brigatti M.F., Drits A., Eberl D.D., Formoso M.L.L., Galan E., Merriman R.J., Peacor D.R., Stanjek H. & Watanabe T. 2002: Report of the AIPEA nomenclature committee for 2001: order, disorder and crystallinity in phyllosilicates and the use of the "Crystallinity Index". *Clay Miner.* 37, 389–393.

Güven A., Karabulut A., Tezcan Ü.Ş. & Balkaş Ö. 1982: Stratigraphy of the Palaeozoic formations and the facies analysis of Hazro formation in the area of Hazro Anticline. *Turkish 6th Petroleum Congress*, *Proc.*, 11–21 (in Turkish).

Hunziker J.C., Frey M., Clauer N., Dallmeyer R.D., Fredrichsen H., Flehmig W., Hochstrasser K., Roggviler P. & Schwander H. 1986: The evolution of illite to muscovite: mineralogical and isotopic data from the Glarus Alps, Switzerland. *Contr. Mineral. Petrology* 92, 157–180.

Inglès M. & Anadón P. 1991: Relationship of clay minerals to depositional environment in the non-marine Eocene Pontils Group, SE Ebro Basin (Spain). *J. Sed. Petrology* 61, 926–939.

Inglès M. & Ramos-Guerrero E. 1995: Sedimentological control on the clay mineral distribution in the marine and non-marine Palaeogene deposits of Mallorca (Western Mediterranean). *Sed. Geol.* 94, 229–243.

Kellog H.E. 1960: Stratigraphic report, Hazro area, Petroleum District V, SE Turkey. *Amer. Overseas Petroleum (AMOSEAS) Report*, 126/1, 42.

Köylüoğlu M. 1986: Chronostratigraphy, microfacies and microfossils of the autochthonous units of the SE Anatolia. [Güneydoğu Anadolu otokton birimlerinin kronostratigrafi, mikrofasiyes ve mikrofosilleri.] *Turkish Petroleum Corporation Res. Center, Educational Publ*. 9, 53 (in Turkish).

Krumm S. 1996: WINFIT 1.2: version of November 1996 (The Erlangen geological and mineralogical software collection) of WINFIT 1.0: a public domain program for interactive profile-analysis under WINDOWS. XIII Conference on Clay Mineralogy and Petrology, Praha, 1994. *Acta Univ. Carolinae Geol.* 38, 253–261.

Kübler B. 1968: Evaluation quantitative du métamorphisme par la cristallinité de l'illite. *Bull. Cent. Rech. Pau SNPA* 2, 385–397.

Lebküchner R.F. 1976: Beitrag zur Kenntnis des Palaozoischen Kerns der Antiklinale von Hazro in Südost-Anatolien. *Miner. Res. Explor. Inst. Turkey Bull.* 86, 1–12.

Merriman R.J. 2005: Clay minerals and sedimentary basin history. *Eur. J. Mineral.* 17, 7–20.

Merriman R.J. & Frey M. 1999: Patterns of very low-grade metamorphism in metapelitic rocks. In: Frey M. & Robinson D. (Eds.): Low-grade metamorphism. *Blackwell Science*, 61–107.

Merriman R.J. & Peacor D.R. 1999: Very low-grade metapelites: mineralogy, microfabrics and measuring reaction progress. In: Frey M. & Robinson D. (Eds.): Low-grade metamorphism. *Blackwell Science*, 10–60.

Moore D.M. & Reynolds R.C. 1997: X-ray diffraction and the identification and analysis of clay minerals. *Oxford Univ. Press*, New York, 1–378.

M.T.A. 2002: 1:500,000 Scale Geological Maps of Turkey. Erzurum and Hatay quadrangles. *General Directorate of Mineral Research and Exploration (MTA)*, Ankara, Turkey.

Özgül N. 1976: Some geological aspects of the Taurus orogenic belt (Turkey). *Bull. Geol. Soc. Turkey* 19, 65–78 (in Turkish, English abstract).

Perinçek D., Duran O., Bozdoğan N. & Çoruh T. 1991: Stratigraphy and paleogeographical evolution of the autochthonous sedimentary rocks in the SE Turkey. *Ozan Sungurlu Symposium*, *Ankara, Proc.*, 274–305.

Reynolds R.C. Jr. 1985: NEWMOD© A Computer Program for the calculation of One-Dimensional Diffraction Patterns of Mixed-Layered Clays: R.C. Reynolds, Jr., 8 Brook Rd., Hanover, NH.

Robinson D. 1987: Transition from diagenesis to metamorphism in extensional and collision settings. *Geology* 15, 866–869.

Schmidt G.C. 1964: Proposed rock unit nomenclature petroleum district V, SE Turkey (Autochthonous Terrain). *Turkish Petroleum Corporation, Archive No: 3955/1*.

Teichmüller M. 1987: Organic material and very low-grade metamorphism. In: Frey M. (Ed.): Low temperature metamorphism. *Blackie & Son*, Glasgow, 114–161.

Tolun N. 1951: Etude géologique du bassin Nord-Est de Diyarbakır. *Miner. Res. Explor. Inst. Turkey Bull.* 41, 65–98.

Tucker M.E. 2001: Sedimentary petrology: An introduction to the origin of sedimentary rocks. *Blackwell Sci.*, 1–262.

Warr L.N. & Rice A.H.N. 1994: Interlaboratory standartization and calibration of clay mineral crystallinity and crystallite size data. *J. Metamorph. Geology* 12, 141–152.

Yahşıman K. & Ergönül Y. 1959: Permian megaspores from Hazru (Diyarbakır). *Miner. Res. Explor. Inst. Turkey Bull.* 53, 92–100 (in Turkish).

Yılmaz E. & Duran O. 1997: Dictionary of stratigraphic nomenclature of the allochthonous and autochthonous units in Southeastern Region, Turkey "Lexicon". [Güneydoğu Anadolu Bölgesi Otokton ve Allokton Birimler Stratigrafi Adlama Sözlüğü (Lexicon).] *Turkish Petroleum Corporation Res. Center, Educational Publ*. 31, 460 (in Turkish).